

REMOVAL OF A BASIC TEXTILE DYE BY RELEASES OF DJEBEL ONK PHOSPHATES

OUISSAM BIBBA^{a*}, SAMIRA MESKI^a, HAFIT KHIREDINE^a

ABSTRACT. The modified natural phosphate of djebel onk was investigated for the removal of cationic textile dye Methylene blue (MB) from aqueous solution. The modified natural phosphate rock powder (MNP) was characterized by means of XRD, IR spectroscopic and thermal analysis. Adsorption studies were carried out under various parameters such as pH, contact time, initial dye concentration and temperature. The equilibrium data were analyzed using Langmuir, Freundlich, Temkin and Dubinin–Radushkevich isotherm models, the results of modeling adsorption of Methylene blue (MB) on modified natural phosphate rock (MNP) show that the Langmuir model present a good coefficient of correlation compared to other models. The kinetics of adsorption were best described by pseudo-second order and the thermodynamic parameters (ΔH° , ΔS° and ΔG°) of the adsorption were also evaluated. The adsorption process was found not-spontaneous and exothermic.

Keywords: Algerian phosphate, adsorption, methylene blue, isotherme

INTRODUCTION

Great quantities of dyes are produced and applied annually in many industries, including industries textile, cosmetic, of paper, of leather, pharmaceutical and food. It is estimated that over 10,000 various dyes and pigments are used industrially and over 7×10^5 tons of synthetic dyes are yearly produced globally. About 10-15% of synthetic dyes are lost during different processes of textile industry [1].

^a Bejaia University, Department of Process Engineering, Environmental Engineering Laboratory, 06000 Bejaia, Algeria.

* Corresponding author: ouissambibba29@gmail.com.

These effluents are rich in dyes and chemicals, some of which are non-biodegradable and carcinogenic and pose a major risk to health and the environment [2]. Several methods of treatment have been used such as coagulation and flocculation [3], biodegradation [4], membrane filtration [5], chemical oxidation [6], ozonization [7] and adsorption [8]. Adsorption is a simple purification technique that is often applied with inexpensive adsorbents in order to clarify waste waters [9]. Among the adsorbents used in processes of discoloration of water we cite: clays [10], activated carbon [11], phosphate [12], hydroxyapatite [13].

Hydroxyapatite ($\text{Ca}_{10}(\text{PO}_4)_6(\text{OH})_2$), a calcium phosphate biomaterial, is a very promising candidate for the treatment of the wastewater. Actually, hydroxyapatite (Hap) can be extremely beneficial in the field of environmental management, due in one part to its particular structure and attractive properties, such as its great adsorption capacities, its acid-base adjustability, its ion-exchange capability and its good thermal stability [14-15]. For these reasons, Hap has been widely used for biomedical and environmental applications. Hap can be synthesized chemically or extracted from natural sources. Natural hydroxyapatite is usually extracted from biological sources or wastes such as mammalian bone (e.g. bovine, camel, and horse) [16], marine or aquatic sources (e.g. fish bone and fish scale), shell sources (e.g. cockle, clam, eggshell, and seashell) [17], and plants and algae and also from mineral sources (phosphate rock) [18].

The principal objective of this work is to study the feasibility of using modified phosphate rock as sorbent for removal of methylene blue dye from aqueous solutions. The choice of this material is based on its inexpensive cost and its abundance in the Algerian ores. The influence of different parameters on the adsorption such as: the contact time, the initial concentration of MB the weight of the adsorbent, the pH of the solvent is studied. The kinetics and isotherms of the adsorption process are also investigated.

2. RESULTS AND DISCUSSIONS

2.1. Characterization of the modified natural phosphate rock

The X-ray diffraction (XRD) patterns of the modified natural phosphate rock (MNP) prepared is represented on the Figure 1. We notice that all the peaks registered in the diagram are characteristic to the hydroxyapatite structure.

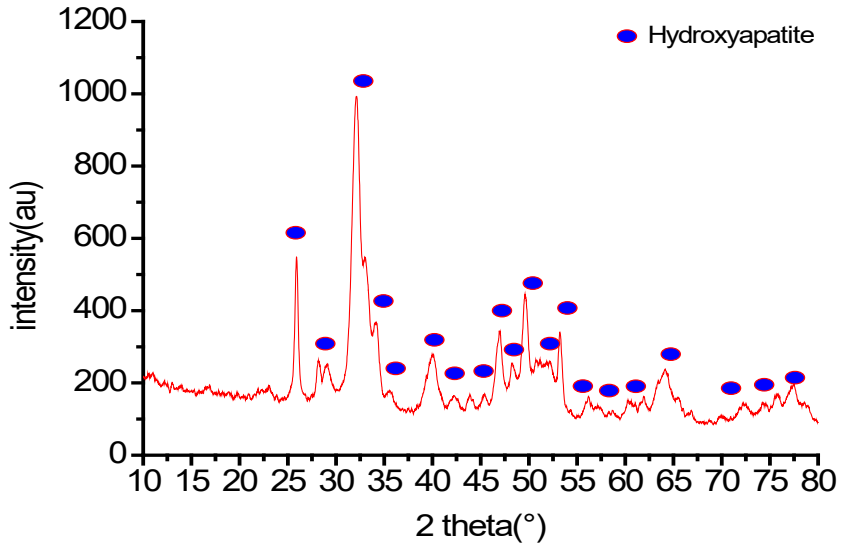


Figure1. X-ray diffraction of the modified natural phosphate rock.

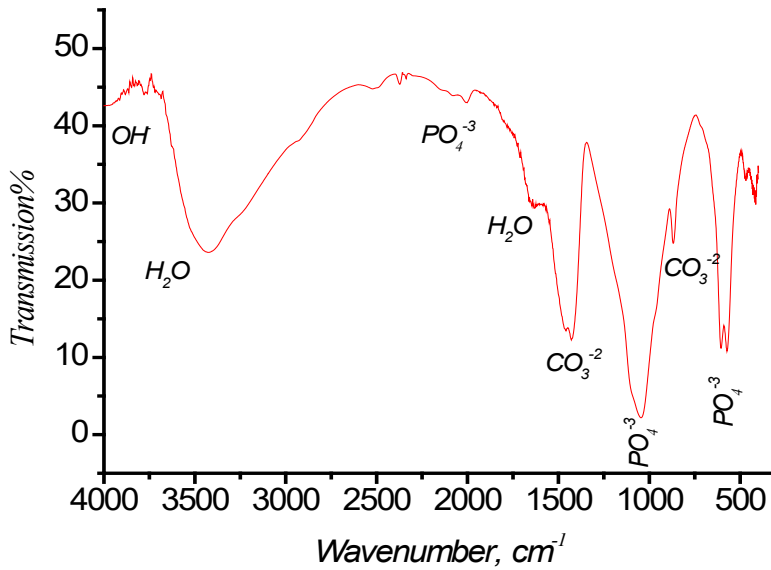


Figure 2. IR spectra of the modified phosphate rock.

The IR spectra of the apatite prepared from phosphate rock of djebel Onk are illustrated in the Figure 2. The bands between 570 - 606 cm^{-1} and 1090-1042 cm^{-1} correspond to the ν_4 and ν_3 PO_4 mode. The band of low intensity obtained at 473 cm^{-1} corresponds to the ν_2 PO_4 mode of the grouping's apatite phosphates. In addition, the bands at 875 and 1425–1450 cm^{-1} are assigned to carbonate vibrations. The bands at 3430 cm^{-1} and 1630 cm^{-1} corresponding, respectively, to the stretching and bending vibration of water molecule used in hydration of powder prepared. Additional band is observed at 3650 cm^{-1} corresponding to OH vibration characteristic to the apatite structure [19].

The TG curve of the modified natural phosphate rock is shown in the Figure 3. We observe that the powder prepared presents three losses of mass, the first is estimated at 6.44% between 20°C-260°C, which corresponds to the dehydration of MNP (departure of the water contained in the pores). The second loss is 4.21%, obtained between 360-496°C attributed to the loss of chemisorbed water. The third loss is obtained at temperature range 500-1000°C. The weight loss in this region is 4.76 % and is due to the decomposition of carbonates, which are already detected by IR spectroscopy. Calcium carbonate reacts to form the oxide of calcium (CaO) according to the reaction:

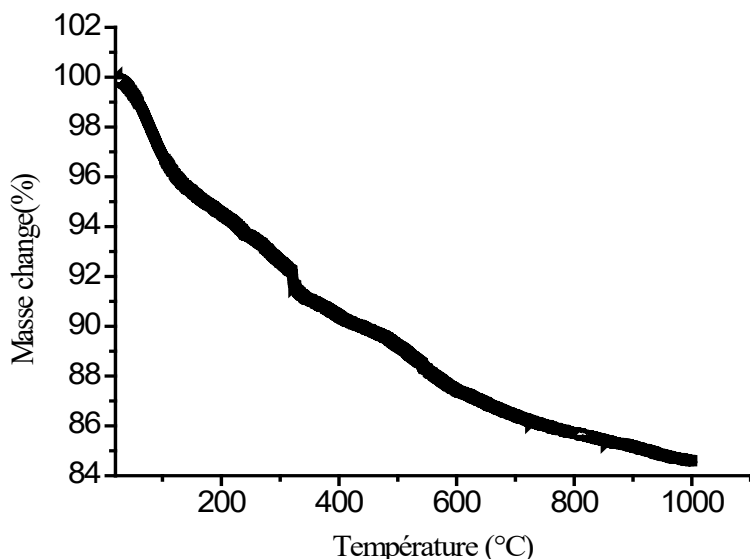
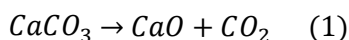


Figure 3. TG analysis of the modified natural phosphate rock.

2.2. Effect of different parameters on MB adsorption

2.2.1. Effect of solution pH

The effect of pH on the removal of methylene blue on the apatite prepared was analyzed in the pH range at 3- 10 at 22 °C, 250 rpm, 1 g of modified natural phosphate rock (MNP) and 250 mL of dye concentration 100 mg/L. The pH was adjusted using 0.1 N NaOH and 0.1 N HCl solutions.

The result in Fig. 4 showed that the removal percentage increase when pH increase from 3 to 9 and decrease for the pH between 9-10. The maximum adsorption of methylene blue was obtained at pH 9.

The low adsorption in acidic medium is due to the repulsion between the positively charged groups of the apatite powder and methylene blue. However, the rapid increase of the removal of MB in the pH range 7-9, can be explained by the attraction force between the positive charge of MB and the negative charge of the powder. These results are similar to those obtained by Khadidja Allam and al (2016) [20] in the adsorption of methylene blue by using hydroxyapatite submitted to microwave irradiation.

According to Liuming Wu and al [21], the reactions responsible for the surface properties of MNP in aqueous solutions are:

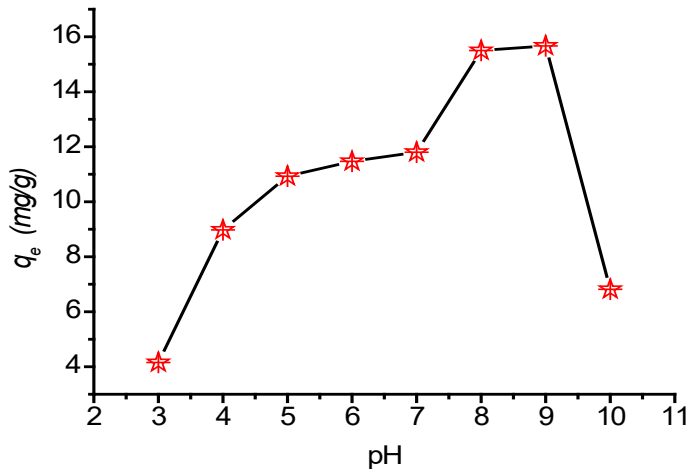
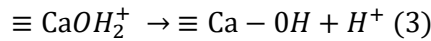
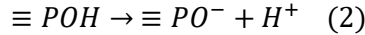


Figure 4. Effect of pH on the adsorption of MB dyes on MNP ($C_0 = 100 \text{ mg. L}^{-1}$, $C_{susp} = 4 \text{ g. L}^{-1}$, $t = 22^\circ\text{C}$).

For the acidic medium, the positively charged (CaOH_2^+) and neutral (P-OH) sites predominate on the MNP surface, giving a positive charge surface for this powder. However, in the basic medium, the neutral (CaOH) and negatively charged (PO^-) species predominated, causing HAP surface to become negatively charged.

The low decrease of the adsorption yield at pH =10 can be associated to the excess of OH^- surrounding the dye by electrostatic attraction, and prevent them from being retained on the anionic sites of the adsorbent.

2.2.2. Effect of initial dye concentration

The evolution of the adsorption percentage of MB in the powder prepared was studied as a function of the initial concentration of MB and contact time. The solution concentration of MB was varied in the range 10- 500 mg/L and the pH solution was adjusted to 9 as it was found to be the optimum pH value from the results of the previous experiment (effect of solution pH).

The curve presented in the figure 5 reveal that the MB adsorption rate is very fast in the first-time contacts with our adsorbent, then reached equilibrium after 60 min. Similar results were obtained by M. Mahmoud and others [22], who studied the adsorption of methylene blue dye onto biopolymer (hydrolyzed oak sawdust (HOSDC)). It was observed that the removal of dye by adsorption on HOSDC was found to be rapid at the initial period of contact time and then to slow down with time. These authors suggest that the phenomenon is due to the forces of attractions between the dye molecule and the adsorbent such as the force of Vander Waals and the electrostatic attractions and as the availability of a large number of sites active on the surface of the adsorbent.

Also, it can be seen from the figure 5 that the adsorption percentage of the MB decrease from 85.76% to 29.87% and 81.5% to 41% at 22 °C and 40°C respectively with the increase in the initial concentration from 10 to 500 mg/L, this can be explained by the competition between the MB molecules for the occupation of actives sites. Generally, an increase in the initial dye concentration in the solution will cause the adsorption sites on the adsorbent surface to become saturated, which eventually leads to a decrease in the removal efficiency.

On the other hand, we observe that for the lower concentrations of MB (10 -200 mg/L), the adsorption percentage values obtained at temperature 22°C is greater than those obtained at 40°C, whereas at high initial MB concentration (500 mg/L) the removal percentage of MB obtained at 40°C is greater than one obtained at 22°C.

REMOVAL OF A BASIC TEXTILE DYE BY RELEASES OF DJEBEL ONK PHOSPHATES

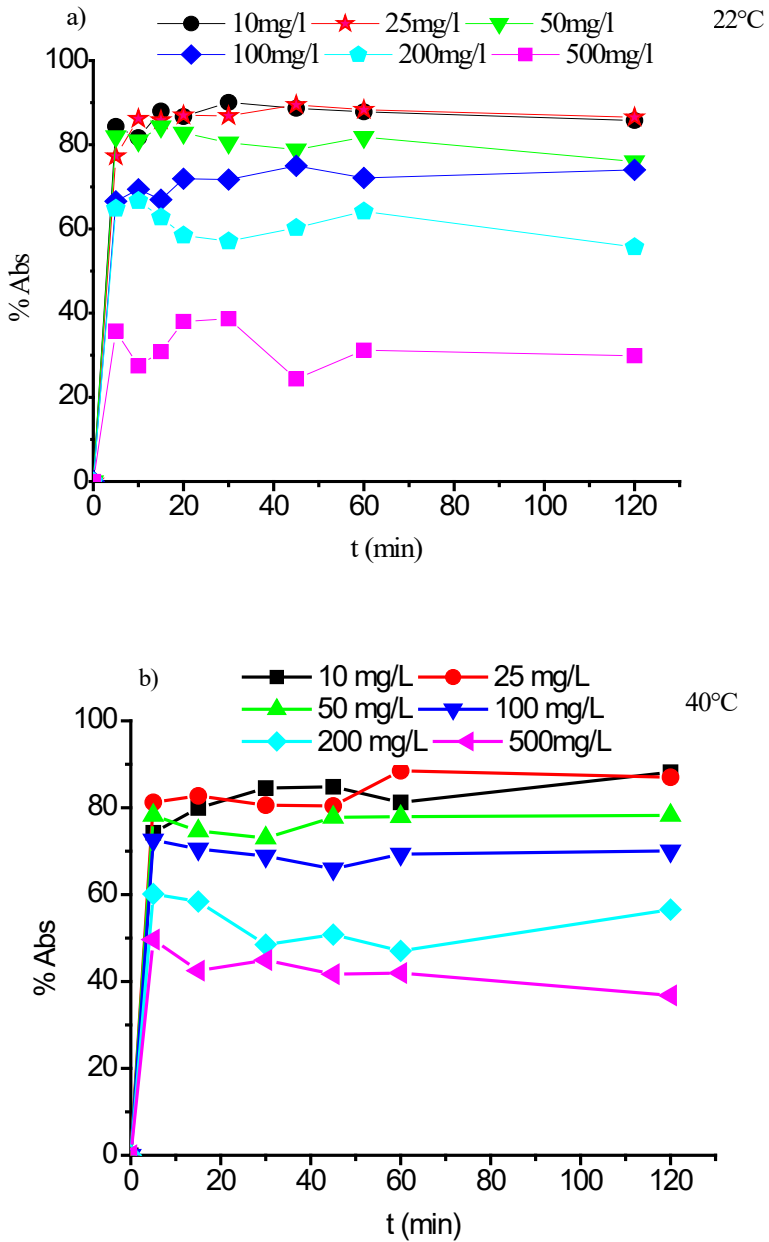


Figure 5. The effect of initial MB dye on percentage dye removal for two temperatures: a, 22°C; b, 40 °C ($pH=9$, $C_{susp} = 4 \text{ g. L}^{-1}$).

2.2.3. Effect of mass of MNP

The effect of the mass of adsorbent on the removal percentage of MB was studied at different masses of MNP (0.5, 1, 2, 4 and 6 g/L), at 22°C, 250 rpm, pH 9 and 250 mL of MB solution (100 mg/L).

The results are presented in Figure 6. As the amount of adsorbent increased between 0.5 to 4 g/L, an increase in dye removal was noticed. These results can be explained by the higher number of active sites available as the adsorbent dose increased, facilitating the adsorption process. For the amount of adsorbent higher than 4g/l, the dye removal decreased. This behavior can be explained: As long as the amount of adsorbent added to the dye solution is low, the cations of the dye can easily access the adsorption sites. Adding adsorbent increases, the number of adsorption sites, but the cations of the dye have more difficulty approaching these sites due to congestion, a large amount of adsorbent can create agglomerations of particles, resulting in reduction of the total adsorption surface and consequently a decrease in the removal percentage [23].

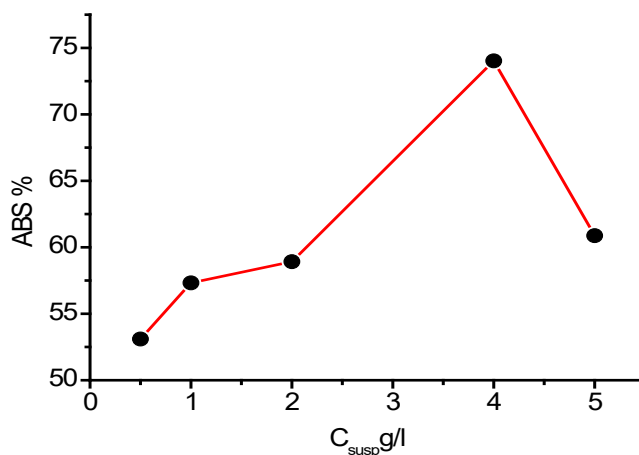


Figure 6. The effect of the concentration of the suspension on percentage dye removal ($pH=9$, $t = 22^{\circ}C$).

2.2.4. Effect of temperature

To investigate the influence of temperature on the adsorption process, five different temperatures were studied (22 °C, 40 °C, 50°C and 60 °C), working at a concentration of 100 mg/L, amount of adsorbent of 4g/L and pH 9 of the solution. The obtained results are presented in Figure 7.

The experimental data presented in Figure 7 show that the increase in temperature determined a decrease in adsorption percentage, indicating that the adsorption of cationic dyes (MB) on MNP is an exothermic process.

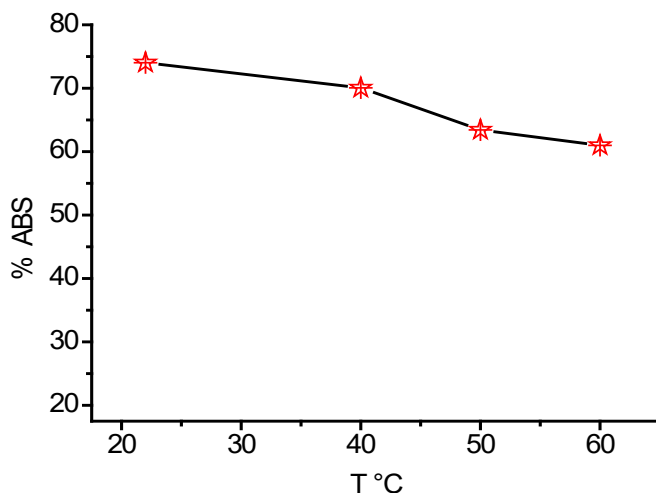


Figure 7. The effect of temperature on percentage dye removal ($pH=9$, $C_{susp} = 4 \text{ g. L}^{-1}$, $C_0 = 100\text{mg.L}^{-1}$)

2.3. Adsorption isotherms

The isothermal sorption curves of MB on the modified phosphate rock at two temperatures are shown in Fig. 8. According to the shapes of the curves, the isotherms corresponding to MB adsorption onto MNP may be classified as L type of the Giles classification [24]. The L type isotherm suggests a relatively high affinity between MB ions and MNP. This also indicates that no strong competition occurs for the adsorption sites between solvent molecules and adsorbate molecules.

All the sorption parameters of the different models; Langmuir, Freundlich, Temkin and Dubinin-Radushkevich are presented in Table 1. The high correlation coefficients were obtained using the Langmuir ($R^2 = 0.998$ at 22°C and 0.969 at 40°C) and Freundlich ($R^2= 0.946$ at 22°C and 0.989 at 40°C) models with a small X^2 . Specifically, the experimental data fitted the Langmuir isotherm model well when the temperature was 22°C while the Freundlich isotherm model gave higher R^2 coefficient and lower X^2 and RMSE values at 40°C .

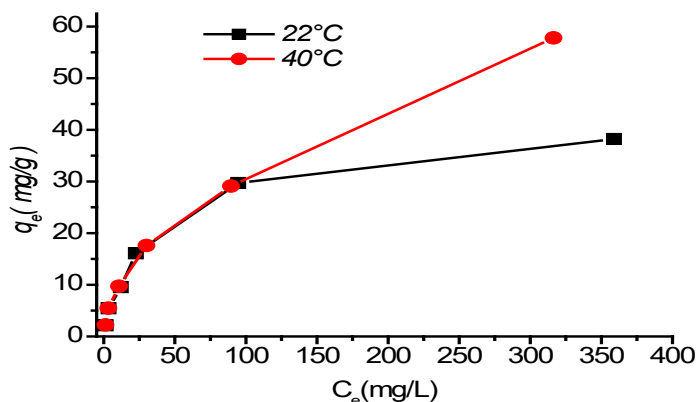


Figure 8. Adsorption isotherms of MB on MNP at different temperatures. 22°C and 40°C ($pH=9$, $C_{susp} = 4 \text{ g.L}^{-1}$, $time = 2 \text{ h}$).

Therefore, at 22°C, methylene blue adsorption onto modified phosphate rock followed a Langmuir model, this suggests that the adsorption process takes place on a homogeneous surface via monolayer sorption with no contact between sorbed molecules.

The dimensionless constants RL were between 0 and 1, and the values for $1/n$ were less than 1, indicating that adsorption was favored. Moreover, the RL constants increased as the temperature increased, indicating that low temperatures promoted MB adsorption. The parameter $1/n$ of Freundlich gives an indication on the validity of adsorption or of the interactions force of adsorption, if the value of $1/n$ is equal to 1, adsorption is linear; if it is higher than 1, adsorption is physical; if it is lower than 1, adsorption is a favorable chemical process [23, 25], all the parameter values $1/n$ found are less than 1 which means that MB dye is favorably adsorbed by the MNP.

The high values of the Temkin model correlation coefficient at 22°C show good linearity, the variation of the Temkin constant relating to the heat of sorption is positive indicating that the adsorption reaction is exothermic [26].

As can be seen in Table 1, the values of Chi-square statistic and RMSE for Dubinin Radushkevich model were 36.739, 11.334 at 22°C and 97.90, 18.83 at 40°C, respectively which are very high in comparison with other models. This reveals that Dubinin Radushkevich model could not describe the experimental isotherm data in the sorption of MB onto MNP.

Table 1. Isotherms parameters by linear method for the sorption of MB by MNP.

	t= 22°C		t=40°C
Langmuir	$R^2=0.998$ $Q_m= 41.442$ mg/g $K_L=0.031$ L/mg $RMSE=1.293$ $X^2=1.032$		$R^2=0.969$ $Q_m=66.401$ mg/g $K_L=0.016$ L/mg $RMSE=4.93$ $X^2=5.53$
Freundlich	$R^2= 0.946$ $K=0.237$ L/mg $1/n=0.461$ $RMSE=5.837$ $X^2=5.290$		$R^2= 0.989$ $K=0.162$ L/mg $1/n=0.556$ $RMSE=1.872$ $X^2=0.588$
Temkin	$R^2= 0.962$ $K_e=0.623$ L/g $B_t=6.841$ $b= 358.51$ j/mol $RMSE=2.400$ $X^2=4.298$		$R^2= 0.868$ $K_e= 0.493$ L/g $B_t=9.262$ $b= 280.96$ j/mol $RMSE=7.112$ $X^2=9.670$
Dubinin-Radushkevich	$R^2=0.723$ $E=0.6031$ Kj /mol $\beta= 1.374 \cdot 10^{-6}$ $Q_m=18.378$ mg/g $RMSE=11.334$ $X^2=36.739$		$R^2=0.642$ $E=0.6868$ Kj /mol $\beta=1.059 \cdot 10^{-6}$ $Q_m=19.915$ mg/g $RMSE=18.83$ $X^2=97.903$

Table 2. R_L values for different concentration.

Dye concentration(mg/l)	Value of R_L	
	t= 22°C	t= 40°C
10	0.843	0.874
25	0.682	0.736
50	0.5178	0.582
100	0.349	0.411
200	0.211	0.258
500	0.096	0.122

The comparison of the maximum monolayer capacity between Langmuir and Dubinin Radushkevich show that Langmuir reveals a better agreement with experimental data. The value of q_m was 41.49 mg/g at 22°C which is more close to experimental capacity (≈ 38 mg/g) in comparison with corresponding Dubinin Radushkevich parameter (q_m) which is almost half (18.37 mg/g) of the experimental capacity. Consequently, Langmuir model better explained the MB sorption experimental data than Dubinin- Radushkevich model.

2.4. Adsorption kinetics

The values of the correlation coefficient (R^2) and adsorbed amount (q_e) determined by plotting the linear form of the first order kinetics presented in Fig. 9 and Table 3, reveal that this model does not adequately describe the adsorption of the methylene blue on the modified phosphate rock.

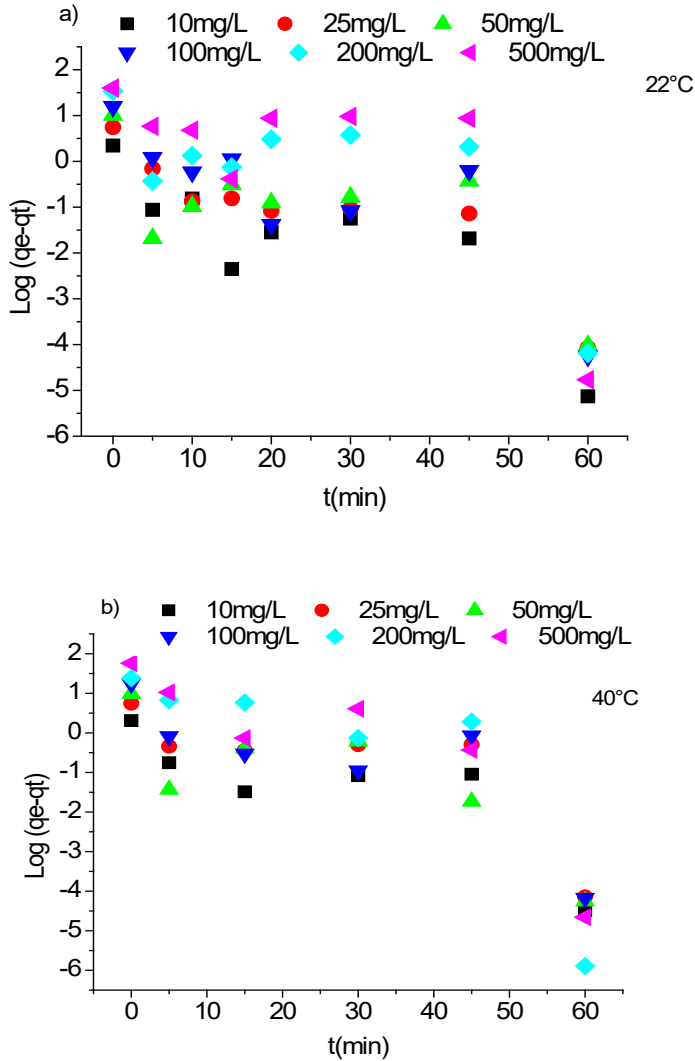


Figure 9. Pseudo- first order model plot for the adsorption of MB onto MNP for two temperatures: a, 22°C ; b, 40°C ($\text{pH}=9$, $C_{\text{susp}}= 4 \text{ g. L}^{-1}$).

Table 3. the pseudo- first order kinetic model parameters of MB dye adsorption onto MNP ($t=22^{\circ}\text{C}$ and $t=40^{\circ}\text{C}$, time = 60mn).

$C_0(\text{mg/l})$ / t	$q_e(\text{mg/g})$		$K_1(\text{min}^{-1})$		$q_e(\text{calculated})(\text{mg/g})$		R^2		RSME		X^2	
	22°C	40°C	22°C	40°C	22°C	40°C	22°C	40°C	22°C	40°C	22°C	40°C
10	2.212	2.046	0.145	0.128	0.589	1.030	0.668	0.653	1.808	1.296	24.180	7.306
25	5.568	5.579	0.135	0.129	1.999	4.540	0.772	0.608	3.995	1.175	16.104	2.200
50	10.264	9.869	0.104	0.142	1.032	2.635	0.433	0.656	10.161	6.582	86.981	17.095
100	15.667	17.412	0.147	0.143	5.544	7.003	0.659	0.643	11.339	12.799	16.093	10.312
200	34.232	24.229	0.133	0.214	13.264	87.841	0.401	0.652	20.620	62.132	14.813	3.248
500	39.894	57.424	0.160	0.191	50.184	69.518	0.496	0.739	10.344	34.503	1.513	742.508

The parameters of the second order kinetics are determined from the linear representation of t/q_t as a function of time (Fig. 10). The values of the parameters are grouped in the Table 4, it is noted that the correlation coefficients for the two temperatures studied are very close to 1. Similarly, the values of the adsorption capacities calculated ($q_{e,cal}$) from the pseudo second order model are in same order of magnitude to those of experimental ($q_{e,exp}$).

Higher correlation coefficient values and smaller RMSE and X^2 were obtained for the pseudo-second-order kinetic model compared to those obtained for the pseudo-first-order kinetic model, indicating that MB adsorption on the MNP adsorbent fitted the pseudo-second-order kinetic model at initial fluoride concentrations ranging from 5 to 15 mg/L. Smaller RMSE values indicated smaller differences between the calculated q_t and experimental q_t values.

Table 4. The pseudo-second-order kinetic model parameters of MB dye adsorption onto MNP ($t=22^{\circ}\text{C}$ and $t=40^{\circ}\text{C}$, time = 60mn).

C_0 (mg/l) / t	$q_e(\text{mg/g})$		$k_2(\text{g/mg.min})$		$q_e(\text{calculated})(\text{mg/g})$		R^2		RSME		X^2	
	22°C	40°C	22°C	40°C	22°C	40°C	22°C	40°C	22°C	40°C	22°C	40°C
10	2.230	2.08	2.002	4.32	2.22	2.084	0.999	0.996	0.063	0.099	0.009	0.180
25	5.593	5.426	0.446	0.248	5.556	5.36	0.999	0.995	0.141	0.282	0.011	0.063
50	10.142	9.68	2.16	0.243	10.131	9.61	0.999	0.998	0.215	0.473	0.022	0.098
100	16.129	17.398	0.120	1.43	16.480	17.37	0.998	1.000	0.969	0.181	0.293	0.006
200	33.222	28.40	0.084	0.012	34.235	27.47	0.995	0.980	2.062	5.620	0.643	7.380
500	36.496	55.26	0.227	0.0143	39.890	54.72	0.970	0.950	6.170	13.91	4.257	16.47

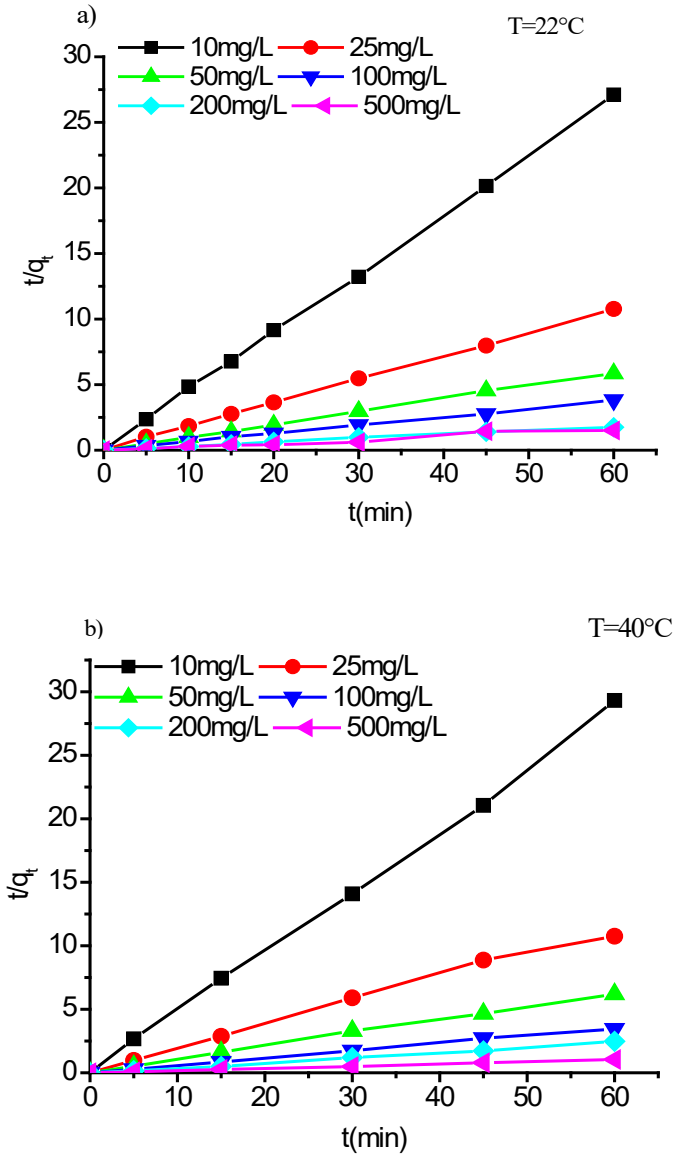


Figure 10. Pseudo-second order model plot for the adsorption of MB onto MNP for two temperatures: a, 22°C; b, 40 °C ($pH=9$, $C_{susp}= 4 \text{ g. L}^{-1}$).

2.5. Thermodynamics studies

The thermodynamic study is represented by the plot $\ln K$ as a function of $1/T$ in the Fig 11. The values of the thermodynamic parameters are presented in the Table 5. The negative value of ΔH (- 14.844 KJ/mole) indicates that the adsorption process is exothermic and confirm the experimental results obtained from the influence of temperature study, which indicate that the adsorption yield decreases with increasing temperature. The positive ΔG values revealed that the adsorption process of MB dye onto MNP was not-spontaneous in nature [27]. The negative value of the entropy variation (ΔS°) suggest that the molecules decrease their randomness at the solid-liquid interface during the adsorption [28].

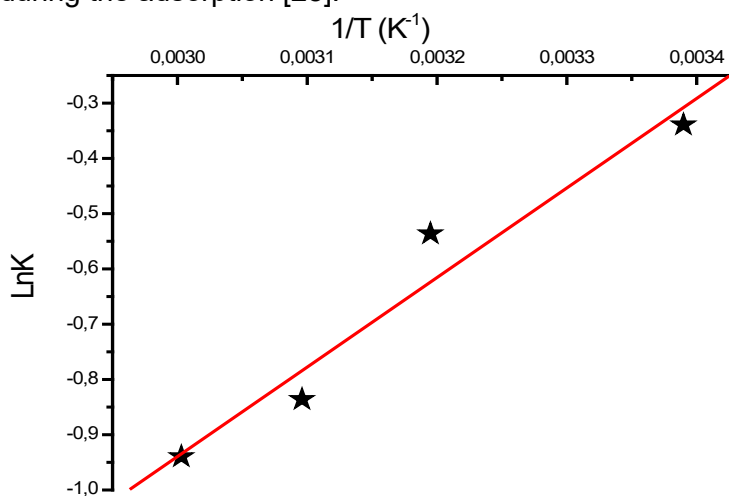


Figure 11. Linear plots of $\ln K$ vs. $1/T$ for methylene blue

Table 5. Thermodynamic parameters for adsorption of MB dye at different temperatures onto MNP.

Temperature (K)	ΔG (KJ/mole)	ΔH° (KJ/mole)	ΔS° (KJ/mole. K)
295	1.085	-14.844	-0.053
313	2.057		
323	2.597		
333	3.137		

Conclusion

The resulting of this study shows the efficiency of methylene blue dye removal in aqueous media by the modified phosphate rock.

The study of the influence of some parameters on the adsorption capacity has shown that the favorable conditions for obtaining a maximum discoloration rate are:

- Concentration of the phosphate suspension $C_{\text{susp}}=4 \text{ g.L}^{-1}$
- pH of the solution = 9
- agitation speed $\omega=250 \text{ rpm}$.
- Temperature $t=22^{\circ}\text{C}$

The adsorption isotherm of MB on MNP for the two-temperature studied (22°C , 40°C) follows the Langmuir and Freundlich models respectively.

The kinetic data is analysed using pseudo first-order and pseudo second-order equations. The experimental data was fitted very well with the pseudo second-order kinetic model.

The negative ΔH° and ΔS° values and positive ΔG° value associated with the adsorption of MB on MNP suggested that the process was exothermic and unspontaneous.

3. MATERIALS AND METHODS

3.1. Adsorbent

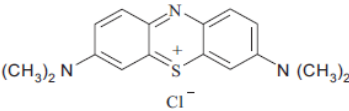
The adsorbent used in this work was the modified phosphate rock of Djbel Onk ores (Kef ESNOUN bir el ater Tebessa) in Algeria. They were repeatedly washed several times with tap water followed by distilled water and then were dried in oven at 100°C for 24 hours. Phosphate rock are crushed and powdered at different fraction. Only the powder of the fraction between 100 and 400 nm grain size, rich in natural phosphate was used in this study.

This powder was totally dissolved in the HNO_3 solution at $\text{pH}=2$ under continuous agitation using a magnetic stirrer for 2 hours at room temperature to obtain calcium and phosphorus precursors. The filtrated solution was then aged for 24 hours after being precipitated with a concentrated ammonium hydroxide solution NH_4OH at room temperature. The precipitate obtained is recovered by a 2nd filtration, washed with distilled water and then dried in an oven at 100°C for 24 hours [18].

3.2. Adsorbate

The adsorbate used in this study is the Methylene blue obtained from Aldrich sigma. The chemical structure and the characteristic of this dye is illustrated in the Table 6.

Table 6. Physicochemical characteristics of the Methylene blue.

Name	Chemical structure	Nature	MW (g.mol ⁻¹)	λ_{\max} (nm)
Methylene blue		Cationic	319.85	664

3.3. Characterization of the adsorbent

The powder (MNP) obtained was characterized by various methods such as:

- X-ray diffraction (XRD) used the PHILLIPS X pert proof, analytical, system MPD diffractometer with Cu K α radiation.
- IR using a Shimadzu-8300 interferometer and with adopting the KBr technique 2 mg of the dried sample powder was compacted with 300 mg of potassium bromide using pressure, the measurements were run in the wave number range from 400 to 4000 cm⁻¹.
- The thermal analysis TGA using a thermogravimetric analyzer (LINSEIS STA-PT 1600) heating was performed in a platinum crucible from 25°C to 1000°C at a heating rate of 10°C/min in a stream of nitrogen.

3.4. Adsorption tests

Stock solution of 1g/L of methylene blue (MB) was prepared by dissolving appropriate amount of this dye in distilled water, and the used concentrations were obtained by dilution. Adsorption experiments were carried out in the batch reactors (500 mL Erlenmeyer) containing various amounts of modified natural phosphate as adsorbent and 250 mL of methylene blue solutions having different concentrations (10, 25, 50, 100, 200 and 500 mg/L) and pH (3–10). The pH solution was adjusted with HCl (0.1M) and NaOH (0.1M).

In order to study the effect of the temperature on the adsorption, five adsorption temperatures (22, 40, 50 and 60 °C) were studied. The mixture was well agitated using a shaker 250 rpm until reaching the equilibrium. Preliminary experiments had shown that the equilibrium adsorption was obtained before 2 hours and for agitation speed of 250 rpm. After this time, the samples were filtered by a Millipore membrane filter type 0.45 μm , and the concentrations of the dyes were analyzed using UV–vis spectrophotometer (ICE 3000 SERIE SAA S) by monitoring the absorbance changes at a wavelength of maximum absorbance of methylene blue (664 nm). All experiments were performed in triplicate and experimental errors were found below 5%.

The adsorbed quantity (q_e) and the removal percentage (Y %) were calculated using the following equations:

$$q_e = \frac{(C_0 - C_e) \cdot V}{m} \quad (4)$$

$$Y(\%) = \frac{(C_0 - C_t) \cdot 100}{C_0} \quad (5)$$

Where C_0 , C_t and C_e represent, respectively, the dye concentrations (mg/L) in the initial solution, at time t and at the equilibrium, respectively, V is the volume of the dye solution (L) and m is the amount (g) of the sorbent used in the reaction mixture.

3.5. Adsorption isotherm models

Equilibrium adsorption studies were performed to determine the maximum MB adsorption capacities of MNP. Langmuir, Freundlich, Temkin and Dubinin-Radushkevich isotherm models were used to fit the equilibrium adsorption data of MB, onto MNP.

3.5.1. Langmuir model

The Langmuir isotherm is based on monolayer adsorption onto a surface with a finite number of adsorption sites. This model assumes that adsorption energies on the surface are uniform and that there is no adsorbate transmigration in the surface plane [29]. The Langmuir model is represented by the following equation:

$$q_e = \frac{K_L q_m C_e}{1 + K_L C_e} \quad (6)$$

The Langmuir parameters models were given by transforming the equation (6) in its linear form:

$$\frac{C_e}{q_e} = \frac{C_e}{q_m} + \frac{1}{q_m K_L} \quad (7)$$

Where C_e is the equilibrium concentration (mg/L), q_e is the equilibrium adsorption amount (mg/g), q_m is the maximum adsorption capacity (mg/g) and K_L is the Langmuir constant (L/mg).

$$R_L = \frac{1}{1 + k_L C_0} \quad (8)$$

A factor of separation $R_L > 1$ indicates that adsorption is unfavorable, if $R_L = 1$ adsorption is known as linear, adsorption is known as favorable when $0 < R_L < 1$, and a null factor of separation ($R_L = 0$) indicates that adsorption is irreversible [22].

3.5.2. Freundlich model

This model is based on multilayer adsorption. In this model, the mechanism and the rate of adsorption are functions of the constant n and K_F [26]. The Freundlich isotherm can be expressed as follows:

$$q_e = K_F C_e^{1/n} \quad (9)$$

The linear form of Freundlich is given by this equation:

$$\ln q_e = \ln K + \frac{1}{n} \ln C_e \quad (10)$$

Where K_F is the constant of Freundlich (L/mg) and n is a constant depicting the adsorption intensity.

3.5.3. Temkin model

The Temkin isotherm accounts that the heat of adsorption of all molecules in the cover layer decreases linearly with coverage due to the decrease in adsorbent-adsorbate interactions, and adsorption of Temkin isotherm is characterized by a uniform distribution of surface binding energies [11]. The Temkin isotherm is expressed by this equation:

$$q_e = \frac{RT}{b} \ln (K_e \cdot C_e) \quad (11)$$

The linear form of Temkin isotherm is presented as follows:

$$q_e = B_t \ln K_e + B_t \ln C_e \quad (12)$$

With $B_t = RT/b$ (J/mol), the constant of Temkin relating to the heat of sorption and K_e (L/g), the adsorption equilibrium constant corresponding to the maximum binding energy.

3.5.4. Dubinin-Radushkevich model

Dubinin–Radushkevich isotherm is generally applied to express the adsorption mechanism with a Gaussian energy distribution onto a heterogeneous surface [30]. The model is given by the following equation:

$$q_e = q_m \exp(-\beta \varepsilon^2) \quad (13)$$

The equation (13) can be linearized in form:

$$\ln q_e = \ln q_m - \beta \varepsilon^2 \quad (14)$$

With q_m , theoretical maximum capacity of adsorbate adsorbed on the surface of the solid and ε potential of Polanyi, corresponding to:

$$\varepsilon = RT \ln \left(1 + \frac{1}{C_e} \right) \quad (15)$$

The constant β represents the adsorption of the molecule on the adsorbent following its transfer since the solution. β and activation energy E (Kj/mol) is used to estimate the adsorption process, are bound by the following relation:

$$E = \sqrt{\frac{1}{2\beta}} \quad (16)$$

- $E < 8$ kJ/mol : physical adsorption
- $8 < E < 16$ kJ/mol: chemical adsorption.

3.5.5. Error function

The adsorption process is characterized using different kinetics and isotherm models, where by the linear variant of the models that best fitted with the experimental data is usually determined using the coefficient of determination (R^2). In addition, two error functions: residual root mean-square errors (RMSE) and chi-square statistic X^2 test were used to further reinforce the suitability of these models [ref]

$$X^2 = \sum_{i=1}^n \left| \frac{qe_{Exp} - qe_{cal}}{qe_{cal}} \right| \quad (17)$$

$$RMSE = \sqrt{\frac{1}{(n-p)} \sum_{i=1}^n (qe_{Exp} - qe_{cal})_i^2} \quad (18)$$

The subscripts “exp” and ‘calc” show the experimental and calculated values and N is the number of observations in the experimental data. If data from the model are similar to the experimental data, X^2 will be a small number; if they are different, X^2 will be a large number. The small the RMSE value, the better the curve fitting.

3.6. Adsorption kinetic models

The kinetic study of the adsorption process reveals the mechanism of adsorption as well as the mode of solute transfer from the liquid to the solid phase. Pseudo-first-order and pseudo-second-order models were used in this study to fit the kinetics data.

3.6.1. Pseudo-first-order kinetic model

The pseudo-first-order model is presented as follows [31]:

$$\log(q_e - q_t) = \log(q_e) - \frac{K_1}{2.303} \cdot t \quad (19)$$

Where:

K_1 (min^{-1}): is the rate constant of pseudo-first order adsorption.

q_e and q_t (mg/g): denote the amount of dyes adsorbed at equilibrium and at time t , respectively.

3.6.2. Pseudo second order kinetic model

The pseudo-second-order model is presented as follows [32] (Zhang, Z and al, 2011):

$$\frac{t}{q_t} = \frac{1}{K_2 \cdot q_e^2} + \frac{1}{q_e} \cdot t \quad (20)$$

Where K_2 ($\text{mg/g} \cdot \text{min}$) is the rate constant of pseudo-second order adsorption.

3.7. Thermodynamic study

Thermodynamic parameters, such as standard free energy change (ΔG°), standard enthalpy change (ΔH°), and standard entropy change (ΔS°) can be calculated using the following equation [33]:

$$K_e = \frac{q_e}{C_e} \quad (21)$$

$$\ln K_e = \frac{\Delta S^\circ}{R} - \frac{\Delta H^\circ}{RT} \quad (22)$$

$$\Delta G^\circ = \Delta H^\circ - T \Delta S^\circ \quad (23)$$

Where:

K_e : is the thermodynamic equilibrium constant (L/g),

T : is the absolute temperature ($^\circ\text{K}$);

R : is the gas constant ($8.314 \text{ J} \cdot \text{mol}^{-1} \cdot \text{K}^{-1}$).

REFERENCES

1. N. Naghmouchi; k. Nahdi; *Adv. Chem.*, **2015**, *11*, 2321-807.
2. M. Dogan; H. Abak; M. Alkan; *J. Hazard. Mater.*, **2009**, *164*, 172–181.
3. I. Khouni; B.Marrot; PH. Moulin; R. B. Amar; *Desalination.*, **2011**, *268*, 27–37.
4. R. Vidhya; A. J. Thatheyus; *Am. J. Microbiol. Res.*, **2013**, *1(1)*, 10-15.
5. G.Ciardelli; L. Corsi; M. Marcucci; *Resour. Conserv. Recycl.*, **2001**, *31*, 189–197.

6. P.K. Malik; S.K. Saha; *Sep. Purif. Technol.*, **2003**, 31, 241-250.
7. M. Koch; *Chemosphere*, **2002**, 46, 109-113.
8. B.K. Nandi; A. Goswami; M.K. Purkait; *J. Hazard. Mater.*, **2009**, 161, 387–395.
9. S. Pandey; J. Ramontja; *Am. J. Chem. App.*, **2016**, 3, 8-19.
10. A. B. AKarim; B. Mounir; M. Hachkar; M. Bakasse; A. Yaacoubi; *J. Water. Sci.*, **2010**, 23, 375–388.
11. O. Ferrandon; H. Bouabane; M. Mazet; *J. Water. Sci.*, **1995**, 8, 183–200.
12. N. Barkaa; A. Assabbane; A. Nounah; L. Laanab; Y. Aïtlchou; *Desalination.*, **2009**, 235, 264–275.
13. N. Barka ; S. Qourzal ; A. Assabbane ; A. Nounah ; Y. Ait-Ichou ; *J. Saudi Chem. Soc.*, **2011**, 15, 263–267.
14. A. Corami; S. Mignardi; V. Ferrini; *J. Colloid Interface Sci.*, **2008**, 317, 402–408.
15. N.Baraka; Q. Samir; A. Ali; N. Abederrahman; A. Yhya; *J. Environ. Sci.*, **2008**, 20, 1268–1272.
16. S. Meski; H. Khireddine; S. Ziani; S. Rengaraj; M. Silanpaa; *Desalin. Water. Treat.*, **2010**, 16, 1-11.
17. S. Meski; N. Tazibt; H. Khireddine; S. Ziani; W. Biba; S. Yala; D. Sidane; F. Boudjouan; N. Moussaoui; *Water. Sci. Technol.*, **2019**, 80, 1226-1237.
18. S. El Asri; A. Laghzizil; A. Saouiabi; A. Alaouib; K., El Abassi; R. M'hamdi; T. Coradin; *Colloids Surf. A Physicochem. Eng. Asp.*, **2009**, 35, 73–78.
19. A. Chandrasekar; S. Sagadevan; A. Dakshnamoorthy; *Int. J. Phys. Sci.*, **2013**, 8, 1639-1645.
20. K, Allam; A. El Bouari; B. Belhorma; L. Bih; *J Water Resource Prot.*, **2016**, 8, 358-371.
21. L. Wu; W. Frsling; P. W. Schindler; *J. Colloid Interface Sci. Sci.*, **1991**, 147, 178-185.
22. M.M, Abd El-Latif; M. Amal Ibrahim, M. F. El-Kady; *Am. J. Sci.*, **2010**, 6, 267-283.
23. K.M. Kifuani; A.K. Kia Mayeko; PH. N. Vesituluta; B.I. Lopaka; G.E. Bakambo, B.M. Mavinga, J. M. Lunguya, *Int. J. Biol. Chem. Sci.*, **2018**, 12, 558-575.
24. C.H. Giles; A.P. D'Silva; I.A. Easton; *J. Colloid Interface Sci.*, **1974**, 47, 766–778.
25. A. B. Karim ; B. Mounir ; M. Hachkar; M. Bakasse; A. Yaacoubi, *Rev. Des Sci. De L'Eau.*, **2010**, 23, 375–388.
26. O. Hamdaoui; E. Naffrechoux; *J. Hazard. Mater.*, **2007**, 147, 381–394.
27. S. Farrokhzadeh; H. Razmi; N. Sadeghi; E. M. Khosrowshahi; *HHHM.*, **2020**, 1, 8-20.
28. B.K. Nandi; A. Goswami; M.K. Purkait; *J. Hazard. Mater.*, **2009**, 161, 387–395.
29. F. O. Umoh; V. E. Osodeke; I. D. Edem; G. S. Effiong; *OALibj.*, **2014**, 1, 1-9.
30. M. Horsfall; Jnr; A. I. Spiff; A. A. Abia; *J. Korean Chem. Soc.*, **2004**, 25, 969-976.
31. N. Fayoud; S.,Alami Younssi; S. Tahiri; A. Albizane; *J. Mater. Environ. Sci.*, **2015**, 6, 3295-3306.
32. Z. Zhang; L. Moghaddam; Ian. M. O'Hara; O.S. Doherty. William; *Chem. Eng. J.*, **2011**, 178, 122-128.
33. H. ELBoujaady; M. Mourabet; A. EL Rhilassi; M. Bennani-Ziatni; R. El Hamri, A. Taitai; *J. Mater. Environ. Sci.*, **2016**, 7, 4049-4063.